

Krauklis wave initiation in fluid-filled fractures by a passing body wave

M. Frehner¹

¹Geological Institute, ETH Zurich, Sonneggstrasse 5, 8092 Zurich, Switzerland; PH +41 44 632 5468; FAX +41 44 632 1030; email: marcel.frehner@erdw.ethz.ch

ABSTRACT

Krauklis waves are a special wave mode bound to and propagating along fluid-filled fractures. They are of great interest because when propagating back and forth a fracture, they may fall into resonance and emit seismic signals with a characteristic frequency. This resonant behavior can lead to strongly frequency-dependent propagation effects for seismic waves and may explain seismic tremor generation in volcanos or affect micro-seismic signals in fractured fluid reservoirs. All existing studies assume a Krauklis wave initiation inside a fracture, for example by hydro-fracturing. Here, Krauklis wave initiation by an incident plane P-wave is studied. The P-wave is scattered at the fracture, but also, two Krauklis waves are initiated, one at each fracture tip (i.e., diffraction-points of the fracture). The initiation of Krauklis waves strongly depends on the fracture orientation with respect to the incident P-wave. High-amplitude Krauklis waves are initiated at moderate (12° – 40°) and high ($>65^\circ$) incident angles with a distinct gap at around 50° . The initiated Krauklis waves are only visible within, but not outside the fracture. Nevertheless, the fact that P-waves can initiate Krauklis waves has important implications for earthquake signals propagating through fluid-bearing fractured rocks (volcanic areas, fluid-reservoirs) or for active seismic surveys in fractured reservoir situations.

INTRODUCTION

The presence of fluids in reservoir rocks has major effects on the propagation of seismic waves, for example dispersion and frequency-dependent attenuation (Biot, 1962; White, 1975; Quintal et al., 2011). Existing effective medium theories, for example the Biot-theory (Biot, 1962) or the squirt-flow theory (Mavko and Jizba, 1991; Dvorkin et al., 1995) describe some of these effects successfully for the case of porous rocks such as sandstone. However, these theories have more difficulties describing fracture-related phenomena. One such phenomenon of particular interest is the so-called Krauklis wave (also Stoneley guided wave), which is a special wave mode that is bound to and propagates along fluid-filled fractures. It is highly dispersive with very low phase velocity at low frequencies (Ferrazzini and Aki, 1987; Korneev, 2008). Krauklis waves are of great interest because when propagating back and forth along a crack they can fall into resonance and emit a seismic signal with a characteristic frequency. Research on Krauklis waves became popular because this

resonance effect was used by Aki et al. (1977), Chouet (1988) and Chouet (1996) to explain long-period volcanic tremor signals recorded before volcanic eruptions and can potentially be used for eruption forecasting. Similar to volcanic areas, Krauklis waves may be of great importance in any other fluid-bearing rock containing fractures, for example in fractured hydrocarbon reservoirs, geothermal systems, or for CO₂-sequestration. In particular, Krauklis waves are relevant for hydrofracturing and micro-seismicity applications, as they are the predominant wave mode in fractures (Korneev, 2010) and can be induced by fracture opening events induced by fluid overpressure (Ferrazzini et al., 1990).

The dispersion behavior of Krauklis waves is well studied analytically (Ferrazzini and Aki, 1987; Ashour, 2000; Korneev, 2008; Korneev, 2010; Korneev, 2011), but only for simple geometries (infinitely long and straight fractures or a layered medium in the case of Korneev, 2011). On the other hand, numerical studies (Chouet, 1986; Yamamoto and Kawakatsu, 2008; Frehner and Schmalholz, 2010) are rare and do also not include complex geometries. All of these studies assume that Krauklis waves are initiated inside the crack, for example by hydrofracturing (Ferrazzini et al., 1990). However, whether Krauklis waves can be initiated by a body wave passing a fluid-filled fracture has major implications for earthquake signals propagating through fluid-bearing fractured rocks (e.g., volcanic areas, fluid-reservoirs) or for active seismic surveys in fluid reservoir settings. Korneev et al. (2009) states: “*It is likely that Stoneley guided wave [i.e., Krauklis wave] is a key phenomenon which might explain observed frequency-dependent and nonlinear behavior of fluid reservoirs.*”, and Korneev (2010) emphasizes “*the importance of including these wave effects into poroelastic theories.*” However, only if Krauklis waves are indeed initiated by body waves, they are relevant and their effect worth to be upscaled and integrated into effective medium theories. Studying the possible initiation of Krauklis waves by a passing P-wave is the scope of the presented work.

NUMERICAL SIMULATION METHOD AND SETUP

The propagation of Krauklis waves is a multi-scale phenomenon. The fracture thickness is orders of magnitude smaller than the wavelength of Krauklis waves or of seismic body waves propagating through a fractured reservoir and the whole reservoir represents yet another length-scale. For numerical simulations, this “*presents a major computational challenge*” (Korneev, 2008). However, Frehner and Schmalholz (2010) presented a finite-element (FE) study demonstrating the capability to deal with this multi-scale phenomenon. The same FE method as in Frehner et al. (2008) and Frehner and Schmalholz (2010) is adapted here to study the initiation of Krauklis waves by a passing P-wave. The employed FE algorithm solves the visco-elastic wave equation in two dimensions. The unstructured triangular mesh allows accurately resolving and discretizing the fracture. The discretization in time is done by an implicit finite-difference scheme (Newmark, 1959). For solving the linear system of equations the standard direct solver provided by MATLAB is used.

The numerical setup shown in Figure 1 consists of a thin water-filled elliptical fracture with 2 m length and an aspect ratio of 0.003 embedded in the homogeneous

surrounding material. The fracture is inclined with respect to the incident plane P-wave by an angle α . The incident plane P-wave pulse has the shape of the second derivative of a Gaussian (i.e., Ricker wavelet) with a dominant wavelength of 1.26 m and a dominant frequency of 1815 Hz. The used material parameters are listed in Table 1. The surrounding material is purely elastic (i.e., dynamic viscosity equal to zero) and the water in the fracture is elastic in its bulk (volume) deformation behavior and viscous in its deviatoric (shear) deformation behavior. The seismic signal (particle displacement) is recorded by a virtual receiver line running parallel to the long axis of the fracture. This receiver line is centered in the fracture and therefore also records the seismic signals inside the fracture.

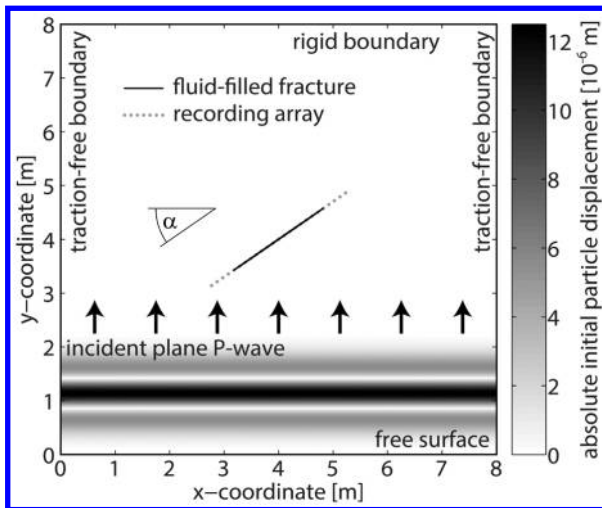


Figure 1. Model setup for studying Krauklis wave initiation by a passing plane P-wave. The boundaries are far enough away from the central fracture in order not to see any reflections from the boundaries in the analyzed seismograms.

Table 1. Material parameters for numerical simulations.

Material parameter	Solid (rock)	Fluid (water)
Elastic bulk modulus, K	5 GPa	2.2 GPa
Elastic shear modulus, μ	6 GPa	0 Pa
Dynamic viscosity, η	0 Pa s	$1 \cdot 10^{-3}$ Pa s
Density, ρ	2500 kg/m ³	1000 kg/m ³
P-wave velocity, V_P	2280 m/s	1483 m/s
S-wave velocity, V_S	1549 m/s	-
Krauklis wave velocity at dominant frequency, V_K	552 m/s (at 1815 Hz) (Korneev, 2008)	

RESULTS

As an example, Figure 2 shows four simulation snapshots of the simulation with an inclination angle $\alpha=45^\circ$. Only secondary waves are visible because the theoretical incident P-wave field is subtracted from the total wave field. In this simulation (and similar ones with different α) the most obvious secondary waves are the body waves, which are scattered at the fracture and diffracted at the two fracture tips. No obvious Krauklis waves can be observed in Figure 2.

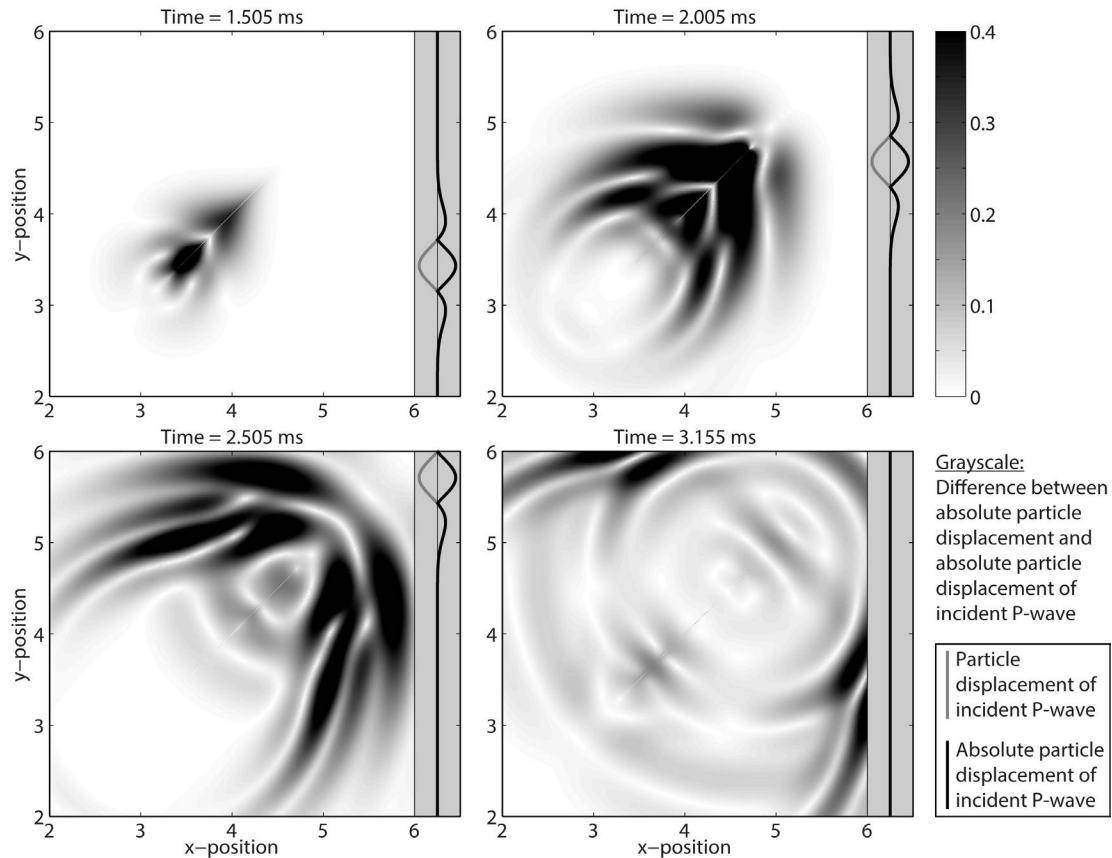


Figure 2. Snapshots of a simulation with inclination angle, $\alpha=45^\circ$. The incident P-wave is propagating from the bottom of the model towards the top and its profile is shown in the gray sidebars of each subfigure. In each simulation snapshot the signal of the incident P-wave is subtracted from the total absolute particle displacement for better visibility of the scattered and diffracted waves.

Figure 2 does not clearly reveal the displacement field inside the fracture, because the fracture is too thin. To also have a look inside the fracture, Figure 3 displays seismic time sections along the receiver line of three simulations with different inclination angle. Only the displacement parallel to the length of the fracture is shown, because in fracture-perpendicular direction no Krauklis waves are visible in the seismograms. In all seismic sections only the incident P-wave and two Krauklis waves can be identified. All other possible wave types are not initiated. There are two Krauklis waves initiated by the incident P-wave, one at each fracture tip corresponding to the two diffraction points of the fracture. The two initiated waves have opposite polarity, which is well recognizable for low inclination angles (Figure 3a). From the fracture tip, the Krauklis waves propagate along the fracture with a very low velocity (Table 1), which is evident from the slope in the seismic sections. The strong dispersion of the Krauklis waves can be observed in Figure 3. The phase velocity, which is well predicted by the analytical value, is considerably larger than the group velocity. In other words, the envelope of the Krauklis wave signal propagates slower than the individual peaks and troughs.

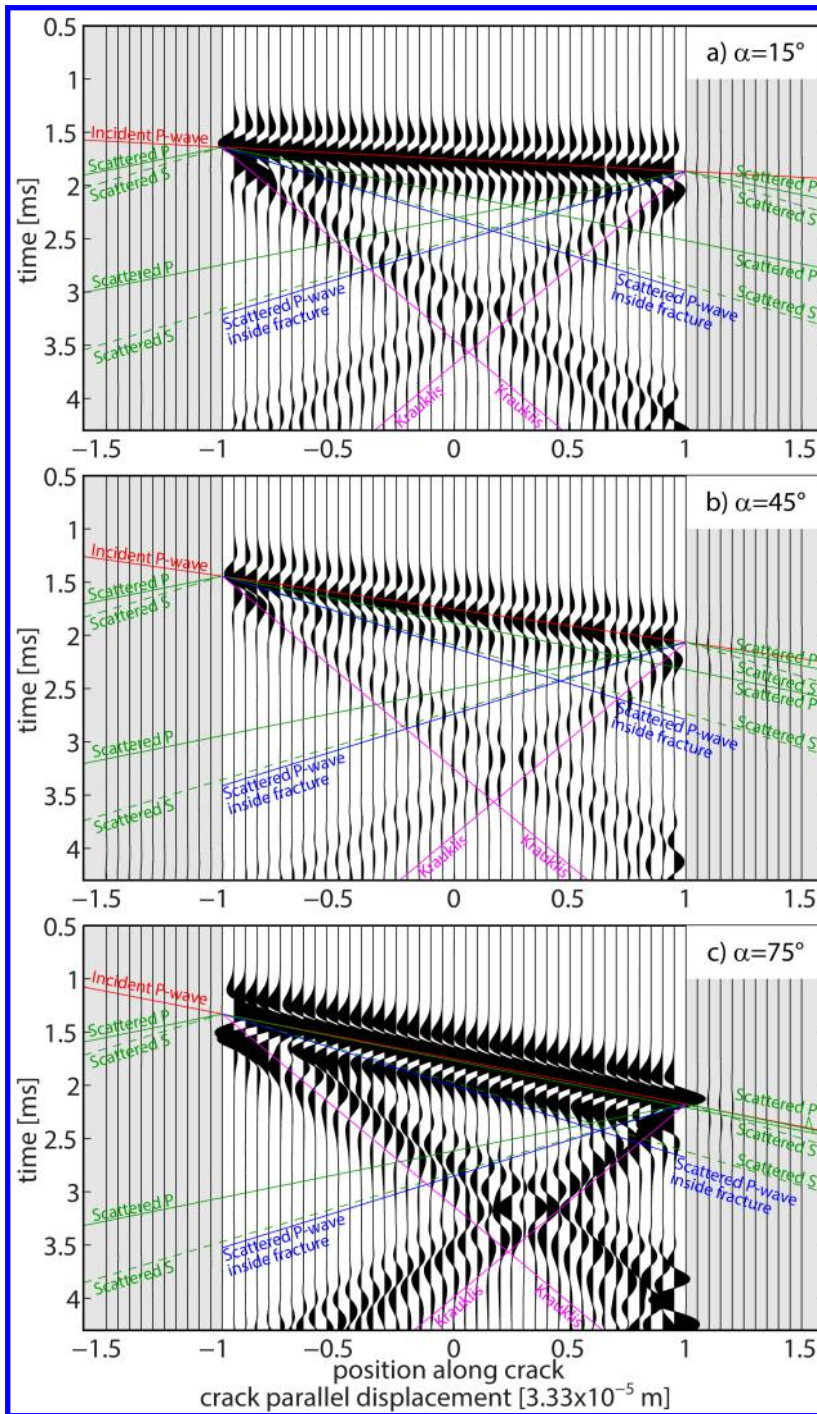


Figure 3. Seismic time sections of the receiver line shown in Figure 1. Displayed is the particle displacement in fracture-parallel direction, from which the theoretical incident P-wave signal is subtracted (i.e., only the differential displacement is shown). The three panels show different inclination angles α (i.e., 15° , 45° , and 75°). The straight lines indicate theoretical phase velocities of different waves, i.e. the incident wave and waves initiated at the fracture tip. The gray shaded areas on either side of each panel indicate receivers outside the fracture; the white central area indicates receivers within the fracture.

Figure 4 shows the amplitude of the initiated Krauklis waves. Close to the fracture tips the Krauklis waves interfere with the incident P-wave (Figure 3). Therefore, Figure 4 only shows Krauklis wave amplitudes along the central part of the fracture. Where the two initiated Krauklis waves pass each other, a distinct interference pattern occurs (Figure 4a). It consists of a central low, which is due to the opposite polarity of the two Krauklis waves, flanked by two high amplitude values. This interference pattern occurs slightly on the far side of the crossing point between

the two theoretical Krauklis wave phase velocities radiating from the two fracture tips (indicated as a black line in Figure 4a). This slight shift is an effect of the strong Krauklis wave dispersion. The initiation of Krauklis waves strongly depends on fracture orientation. For inclination angles smaller than around 12° and between around 40° and 65° , the mean Krauklis wave amplitude is more than 10 times smaller than the amplitude of the incident P-wave and can therefore be considered negligible for these angles. The largest Krauklis wave amplitudes are initiated when the propagation direction of the P-wave is parallel to the fracture (i.e., $\alpha=90^\circ$).

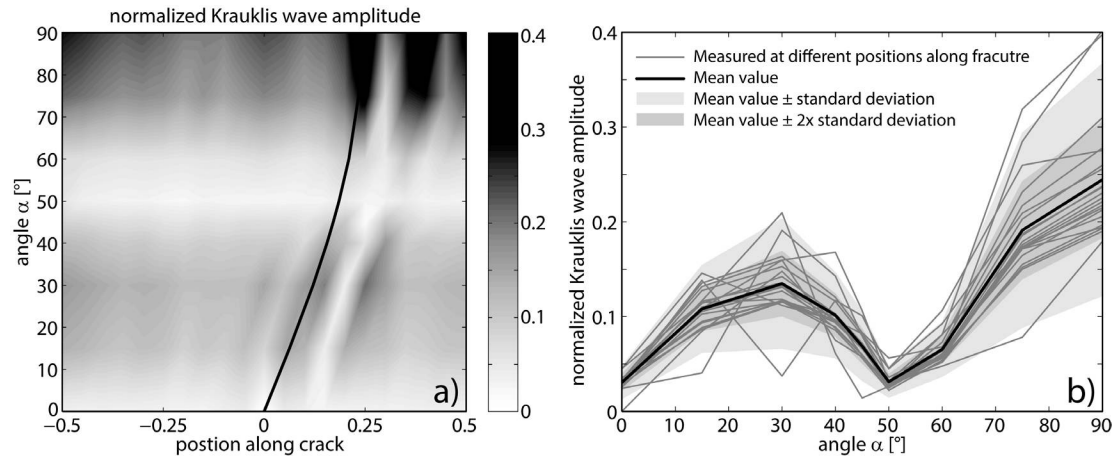


Figure 4. a) Krauklis wave amplitude as a function of the recording position along the fracture and the inclination angle of the fracture, α , measured in fracture-parallel direction and normalized with the maximum amplitude of the incident P-wave. Black line: Crossing-point between the two analytical Krauklis wave phase velocities radiating from the two fracture tips (see Figure 3). b) Same as a) but with all recordings along the fracture plotted on top of each other with the mean value and standard deviation for every inclination angle.

DISCUSSION

In all seismic sections (Figure 3) the Krauklis waves are the only detectable initiated waves indicating that the Krauklis wave is indeed the predominant wave mode in fractures, as suggested by Korneev (2010). However, this is only true when looking at the seismic wave field within the fracture. Outside the fracture (Figure 2) it is difficult to detect the Krauklis waves in the presented study. However, when the Krauklis wave reaches a fracture tip or an intersection with another fracture, part of the Krauklis wave is mode-converted into body-waves and emitted into the surrounding rock (Frehner and Schmalholz, 2010). Therefore, Krauklis wave-related seismic signals may also be detected further away from the fractures.

For the studied simplified case of a single fracture a seismic P-wave is capable of initiating Krauklis waves. The initiation happens at the fracture tips, which corresponds to the two diffraction points of a single fracture. In more realistic settings fractures may have uneven surfaces or fractures of different fracture sets may crosscut each other. Therefore, in natural fractured rocks more diffraction points are expected

along the fractures and the potential to initiate Krauklis waves by a passing P-wave is even larger than in the studied case. Another simplification of the presented study is the two-dimensional modeling approach. The results can therefore be applied to extended planar fractures, but care has to be taken when elongated (i.e., cigar-shaped) fractures are considered.

It has been known that Krauklis waves are initiated by a seismic source inside the fracture (Chouet, 1986; Frehner and Schmalholz, 2010), for example by fracture opening events due to hydrofracturing (Ferrazzini et al., 1990). However, the initiation of Krauklis waves by a passing P-wave has more severe implications. For example, teleseismic signals may initiate Krauklis waves in volcanic areas, where magmatic dykes and sills act as waveguides, or commercial seismic sources may trigger Krauklis waves in fractured hydrocarbon reservoirs. In both cases the frequency-dependent propagation effects due to Krauklis wave initiation can modify the seismic signals propagating through the fractured rocks. On the other hand, in hydrofracturing and micro-seismicity applications the seismic source is within the fractured rock body. Even though this case is not accurately represented by the plane P-wave front used in this study, an initiation of Krauklis waves can also be expected. They can carry energy away from the source along fractures and emit it again at the fracture tip (Frehner and Schmalholz, 2010), which then acts as a secondary source. Therefore, Krauklis waves may reduce the accuracy of micro-seismic localizations. Because the initiation of Krauklis waves depends on fracture orientation (Figure 4), modified P-waves propagating through a fractured fluid-saturated rock may carry information about the fracture orientation. One goal of future studies will be to extract this information from seismic recordings.

Once Krauklis waves are initiated, they can repeatedly propagate back and forth along a fracture, which corresponds to a rock-internal oscillatory behavior. The interaction between seismic body-waves and an oscillatory behavior has been studied by Frehner et al. (2009), Huang et al. (2009), Steeb et al. (2010), and Steeb et al. (2012). They all found a strong dispersion of the body-waves in case the oscillatory behavior can be described by a narrow distribution of resonance frequencies. Therefore, it is expected that in the case of relatively constant fracture lengths and apertures, Krauklis waves lead to a strongly frequency-dependent wave propagation behavior for body waves. On the other hand, Steeb et al. (2012) demonstrated that in case the resonance frequencies are evenly distributed the dispersion curve of the rock stays the same, but the peak dispersion and attenuation can be shifted to higher frequencies. Therefore, in the case of strongly varying fracture lengths and apertures, the frequency-dependency for body-wave propagation is expected to be less pronounced, but the dependency on fracture orientation may still remain.

The above mentioned effective medium models of Frehner et al. (2009), Huang et al. (2009), Steeb et al. (2010), and Steeb et al. (2012), which incorporate a rock-internal oscillatory behavior into wave propagation models, are isotropic. However, the presented study demonstrates that the initiation of Krauklis waves strongly depends on fracture orientation. This anisotropy effect needs to be taken into consideration when future effective medium theories are developed for fractured rocks incorporating Krauklis-wave effects.

CONCLUSIONS

Seismic P-waves propagating through a fractured fluid-filled rock can initiate Krauklis waves. The initiation strongly depends on the fracture orientation with respect to the incident P-wave. Almost no Krauklis waves are initiated for small inclination angles and for inclination angles between 40° and 65° ; the strongest initiation occurs when the P-wave propagates parallel to the length of the fracture. Even though the initiated Krauklis waves themselves are only detectable within the fracture, the mode-conversion into body waves at the fracture tips and other diffraction points should allow detecting Krauklis wave-related seismic signals. The initiation of Krauklis waves is expected to lead to a strongly frequency-dependent and anisotropic propagation behavior for body waves, particularly in the case of a single fracture set with constant orientation and length.

ACKNOWLEDGEMENTS

This work was supported by the Swiss National Science Foundation (SNF) project “UPseis” (project no. 200021_143319). Erik H. Saenger, Beatriz Quintal, and Claudio Madonna are greatly acknowledged for their helpful input.

REFERENCES

- Aki, K., Fehler, M., and Das, S. (1977). “Source mechanism of volcanic tremor: Fluid-driven crack models and their application to the 1963 Kilauea eruption.” *Journal of Volcanology and Geothermal Research*, 2, 259–287.
- Ashour, A. S. (2000). “Wave motion in a viscous fluid-filled fracture.” *International Journal of Engineering Science*, 38, 505–515.
- Biot, M. A. (1962). “Mechanics of deformation and acoustic propagation in porous media.” *Journal of Applied Physics*, 33, 1482–1498.
- Chouet, B. (1986). “Dynamics of a fluid-driven crack in three dimensions by the finite-difference method.” *Journal of Geophysical Research*, 91, 13967–13992.
- Chouet, B. (1988). “Resonance of a fluid-driven crack: Radiation properties and implications for the source of long-period events and harmonic tremor.” *Journal of Geophysical Research*, 93, 4375–4400.
- Chouet, B. A. (1996). “Long-period volcano seismicity: Its source and use in eruption forecasting.” *Nature*, 380, 309–316.
- Dvorkin, J., Mavko, G., and Nur A. (1995). “Squirt flow in fully saturated rocks.” *Geophysics*, 60, 97–107.
- Ferrazzini, V., and Aki, K. (1987). “Slow waves trapped in a fluid-filled infinite crack: Implication for volcanic tremor.” *Journal of Geophysical Research*, 92, 9215–9223.
- Ferrazzini, V., Chouet, B., Fehler, M., and Aki, K. (1990). “Quantitative-analysis of long-period events recorded during hydrofracture experiments at Fenton Hill, New-Mexico.” *Journal of Geophysical Research*, 95, 21871–21884.

- Frehner, M., Schmalholz, S. M., Saenger, E. H., and Steeb H. (2008). "Comparison of finite difference and finite element methods for simulating two-dimensional scattering of elastic waves." *Physics of the Earth and Planetary Interiors*, 171, 112–121.
- Frehner, M., Schmalholz, S. M., and Podladchikov, Y. (2009). "Spectral modification of seismic waves propagating through solids exhibiting a resonance frequency: A 1-D coupled wave propagation–oscillation model." *Geophysical Journal International*, 176, 589–600.
- Frehner, M., and Schmalholz, S. M. (2010). "Finite-element simulations of Stoneley guided-wave reflection and scattering at the tips of fluid-filled fractures." *Geophysics*, 75, T23–T36.
- Huang, H. H., Sun, C. T., and Huang, G. L. (2009). "On the negative effective mass density in acoustic metamaterials." *International Journal of Engineering Science*, 47, 610–617.
- Korneev, V. (2008). "Slow waves in fractures filled with viscous fluid." *Geophysics*, 73, N1–N7.
- Korneev, V., Ponomarenko, A. A., and Kashtan, B. M. (2009). "Stoneley guided waves: What is missing in Biot's theory?" *Poro-Mechanics IV*, DEStech Publications, Inc., Lancaster, 706–711, ISBN 978-1-60595-006-8
- Korneev, V. (2010). "Low-frequency fluid waves in fractures and pipes." *Geophysics*, 75, N97–N107.
- Korneev, V. (2011). "Krauklis wave in a stack of alternating fluid-elastic layers." *Geophysics*, 76, N47–N53.
- Mavko, G., and Jizba, D. (1991). "Estimating grain-scale fluid effects on velocity dispersion in rocks." *Geophysics*, 56, 1940–1949.
- Newmark, N. M. (1959). "A method of computation for structural dynamics." *Journal of the Engineering Mechanics Division*, 85, 67–94.
- Quintal, B., Steeb, H., Frehner, M., and Schmalholz, S. M. (2011). "Quasi-static finite element modeling of seismic attenuation and dispersion due to wave-induced fluid flow in poroelastic media." *Journal of Geophysical Research*, 116, B01201.
- Steeb, H., Frehner, M., and Schmalholz, S. M. (2010). "Chapter 19: Waves in residual-saturated porous media." *Mechanics of Generalized Continua: One Hundred Years after the Cosserats*, Springer Verlag, New York, 179–190, ISBN 978-1-4419-5694-1.
- Steeb, H., Kurzeja, P., Frehner, M., and Schmalholz, S. M. (2012). "Phase velocity dispersion and attenuation of seismic waves due to trapped fluids in residual-saturated porous media." *Vadose Zone Journal*, 11, vj2011.0121.
- White, J. E. (1975). "Computed seismic speeds and attenuation in rocks with partial gas saturation." *Geophysics*, 40, 224–232.
- Yamamoto, M., and Kawakatsu, H. (2008). "An efficient method to compute the dynamic response of a fluid-filled crack." *Geophysical Journal International*, 174, 1174–1186.